J. Am. Chem. Soc. 1987, 109, 7362–7373

The Anomeric Effect with Central Atoms Other Than Carbon. 1. Strong Interactions between Nonbonded Substituents in Polyfluorinated First- and Second-Row Hydrides

Alan E. Reed and Paul von Ragué Schleyer*

Contribution from the Institut für Organische Chemie der Friedrich-Alexander-Universität, Erlangen-Nürnberg, D-8520 Erlangen, Federal Republic of Germany.

Received December 30, 1986

Abstract: An ab initio study of all normal valence polyfluorinated compounds F_nAH_m of the elements Be–O and Mg–S has been carried out to the MP2/6-31G*//HF/6-31G* level of theory. The stabilization energies ΔE ($F_nAH_m + (n-1)AH_{m+n} \rightarrow nFAH_{m+n-1}$) are quite large for elements A of intermediate electronegativity (P, C, S), weaker for the more electronegative elements (N, O), and much weaker or even destabilizing for the electropositive elements (Be, B, Mg, Al). The A–F bond length contractions with respect to the monofluorinated species exhibit a significantly different trend, becoming progressively greater with increasing electronegativity (up to A = N). These trends were interpreted with the aid of natural bond orbital (NBO) energetic analysis, which showed that the energetic stabilizations can be entirely attributed to $n_F \rightarrow \sigma^*_{AF}$ negative hyperconjugation, but that the bond length contractions, particularly in the fluoromethane series, are primarily due to electrostatic, charge withdrawal effects. In CF_4, the σ-bonding is found to involve roughly sp^2 hybridization. Finally, it is demonstrated with the aid of NBO analysis that negative hyperconjugation favors *wider* FAF bond angles and thus counteracts the tendency toward smaller FAF angle due to the high p-character of AF bonds. Negative hyperconjugation thus provides an explanation for the bond angles in PF_3 and SF_2 which are wider than the angles in the corresponding hydrides, PH_3 and SH_2.

I. Introduction

Strong electronic interactions can result when two or more substituents are attached to a common center, even though this center, e.g., a methylene group, would appear to be "insulating".[1,2] A comprehensive survey of such interactions between X and Y in XCH_2Y systems revealed stabilizations (evaluated by eq 1) of

$$XCH_2Y + CH_4 \rightarrow CH_3X + CH_3Y \qquad (1)$$

over 10 kcal/mol for all combinations of the first-row substituents, X, Y = NH_2, OH, and F.[1b,2] In contrast, all combinations of second-row groups, X, Y = PH_2, SH, and Cl, failed to show any appreciable energetic effects. This behavior is typical in most other instances as well, where the groups are neither very strong π-donors nor very effective σ-acceptors. Hence, the exceptions are extremely important since bond lengths, bond angles, and conformations are affected strongly by the same effects which govern the interaction energies. "No bond resonance", the "anomeric" or "gauche effect", and "negative hyperconjugation" are terms associated with this phenomenon. Much of the literature in this area has dealt with unusual conformational preferences (e.g., gauche or axial instead of trans or equatorial), but this has tended to obscure the relationship between the stabilization energies and the geometrical variations.

In order to make valid conclusions concerning the relationship between energies and geometries, it is important to seek the origin of these effects in the molecular electronic wave functions. Brockway's classic paper[3] can be said to have initiated this area. He observed that CF bonds are shortened by about 0.06 Å in going from CH_3F to CF_4 and noted that *gem*-difluorocarbons are significantly more stable chemically than monofluorocarbons, which tend to lose HF.[4] Brockway proposed an explanation for the progressive CF bond shortening and strengthening which involved double bond–no bond resonance (eq 2).

$$FCH_2F \leftrightarrow F^- \; CH_2{=}F^+ \leftrightarrow F^+{=}CH_2 \; F^- \qquad (2)$$

The presumed progressive CF bond strengthening with increased fluorine substitution was later verified and quantified.[5] Indeed, Hine found a linear relationship between the number of no bond–double bond resonance structures and the CF bond strengthening in this series.[6] In its molecular orbital formulation, no bond resonance becomes negative hyperconjugation,[7] the delocalization of π-type lone pairs into antibonding orbitals of saturated groups. From a naive viewpoint, however, the no bond–double bond resonance explanation of the progressive bond shortening in the fluoromethanes is self-contradictory, as it should yield no net change in the CF bond order. The average length of a "no bond" and a double bond should be about the same as that of a single bond.

The electrostatic explanation for the bond shortening proposed by various workers[8,9] would seem more reasonable. This involves a progressive charge withdrawal by the fluorines from carbon, resulting in a decreased carbon covalent radius.[9a,h] The possibility therefore arises that the energetic and geometric effects in the fluoromethanes do *not* have a common origin. Furthermore, negative hyperconjugation is not universally accepted as the explanation for the energetic and conformational preference anomeric

---

[1] Leading references to the extensive literature in this area may be found in our earlier papers on anomeric effects: (a) Schleyer, P. v. R.; Kos, A. J. *Tetrahedron* **1983**, *39*, 1141–1150. (b) Schleyer, P. v. R.; Jemmis, E. D.; Spitznagel, G. W. *J. Am. Chem. Soc.* **1985**, *107*, 6393–6394. Also, see: ref 2.

[2] For further discussion of bond separation reactions and geminal interactions, see: Hehre, W. J.; Radom, L.; Schleyer, P. v. R.; Pople, J. A. *Ab Initio Molecular Orbital Theory*; Wiley: New York, 1986; p 356f.

[3] Brockway, L. O. *J. Phys. Chem.* **1937**, *41*, 185–195.

[4] Henne, A. L.; Midgley, T., Jr. *J. Am. Chem. Soc.* **1936**, *58*, 882–884.

[5] Patrick, C. R. *Adv. Fluorine Chem.* **1961**, *2*, 1–34.

[6] Hine, J. *J. Am. Chem. Soc.* **1963**, *85*, 3239–3244.

[7] (a) Lucken, E. A. C. *J. Chem. Soc.* **1959**, 2954–2960. (b) Romers, C.; Altona, C.; Buys, H. R.; Havinga, E. *Top. Stereochem.* **1969**, *4*, 39–97. (c) David, S.; Eisenstein, O.; Hehre, W. J.; Salem, L.; Hoffmann, R. *J. Am. Chem. Soc.* **1973**, *95*, 3806–3807. (d) Albright, T. A.; Burdett, J. K.; Whangbo, M.-H. *Orbital Interactions in Chemistry*; Wiley: New York, 1985; pp 171–182.

[8] (a) Bent, H. A. *Chem. Rev.* **1961**, *61*, 275. (b) Peters, D. *J. Chem. Phys.* **1963**, *38*, 561–563. (c) Shustorovich, E. *J. Am. Chem. Soc.* **1978**, *100*, 7513–7522.

[9] (a) Hehre, W. J.; Pople, J. A. *J. Am. Chem. Soc.* **1970**, *92*, 2191–2197. (b) Wolfe, S.; Whangbo, M.-H.; Mitchell, D. J. *Carbohydr. Res.* **1979**, *69*, 1–26. (c) Pross, A.; Radom, L. *J. Comput. Chem.* **1980**, *1*, 295–300. (d) Roelandt, F. F.; van der Vondel, D. F.; van den Berghe, E. V. *J. Organomet. Chem.* **1975**, *94*, 377–381. (e) Oberhammer, H. *J. Mol. Struct.* **1975**, *28*, 349–357. (f) Typke, V.; Dakkouri, M.; Oberhammer, H. *J. Mol. Struct.* **1978**, *44*, 85. (g) Oberhammer, H. *J. Fluorine Chem.* **1983**, *23*, 147. (h) The significant influence of methyl substituent electronegativity on the carbon covalent radius has been shown by Francl et al. (Francl, M. M.; Hout, R. F.; Hehre, W. J. *J. Am. Chem. Soc.* **1984**, *106*, 563–570).

0002-7863/87/1509-7362$01.50/0

effects not only in the fluoromethanes but in other species as well.[10-16] The alternative explanations involve dipole–dipole interactions,[10] "forbiddenness reduction",[11] "σ-conjugation",[12] and exclusion repulsion interactions.[13,14] Stretwieser et al.[15] argued that negative hyperconjugation is insignificant in the β-fluorethyl anion and favored a polarization interpretation. However, their objections to negative hyperconjugation were based on misleading results due to the use of fixed and inappropriate geometries.[1a,17] Very recently, Smart has reviewed the various conflicting models for the bond contraction and bond strengthening in the fluoromethanes[16] and concluded that the matter remains unresolved.

There is thus an urgent need to examine quantitatively the extent to which these energetic and geometric effects can be attributed to negative hyperconjugation by analyzing the relevant molecular wave functions in relation to chemical bonding concepts. The tool we shall employ for this purpose is natural bond orbital (NBO) analysis,[18] a quantitative method for representing ab initio wave functions in terms of localized Lewis structures. This analysis allows departures from Lewis structures to be evaluated. NBO analysis is quite suitable for the study of hyperconjugative interactions, as such interactions appear in the analysis as donations of electron charge from bond and lone pair NBOs into antibond NBOs by virtue of nonzero density and Fock matrix elements connecting these two sets of orbtials.

In this work, we not only reexamine the "anomeric effect" in the fluorocarbons but also explore the extent to which strong electronic interactions can occur in polyfluorinated species when the central atom is other than carbon. We consider here as central atoms the entire set of di- or higher valent elements of the first two rows of the periodic table, Be, B, C, N, O, Mg, Al, Si, P, and S. This paper concentrates on the interaction energies and the bond length and bond angle effects which result when more than one fluorine is present. The extremely strong stabilizing interactions among fluorine substituents in the fluorocarbons has received much attention, but very little thermochemical information is available for the other members of our set. Benson lists data for F_2O (stabilized by 5 ± 3 kcal/mol relative to FOH: $F_2O + H_2O \rightarrow 2FOH$).[19] Some experimental data for second-row fluorides are available, but most are missing or are of questionable accuracy. In contrast, it is now a routine matter to obtain reliable geometries and energies of entire sets of such molecules by means of ab initio calculations. Indeed, Schlegel has already studied the SiH_nF_{4-n} series comprehensively.[20] Although relationships like eq 1 were used to evaluate the data and quite large stabilizing effects of polyfluoro substituents were found, no particular point of this was made in the paper. A similar comprehensive examination of SiH_nCl_m species by Ho, Binkley, et al.[21] provides data which afford interesting contrasts. In SiH_2F_2 (eq 3) the mutual stabilization of the two fluorines is 8 kcal/mol (about half of the corresponding value of CH_2F_2), but the chlorine interactions in SiH_2Cl_2 (eq 4) are negligible. The same situation is found in CH_2Cl_2.

Table I. Absolute Energies (–au) at First-Row F_nAH_m Species

species	point group	3-21G// 3-21G	6-31G*// 6-31G*	MP2/6-31G*// 6-31G*
BeH_2	$D_{\infty h}$	15.67378[a]	15.76593[a]	15.80320[a]
FBeH	$C_{\infty v}$	114.11411[a]	114.72716[a]	114.93966
F_2Be	$D_{\infty h}$	212.54025[a]	213.67777[a]	214.06251
BH_3	D_{3h}	26.23730[a]	26.39001[a]	26.46423[a]
FBH_2	C_{2v}	124.64675[a]	125.32213	125.56796
F_2BH	C_{2v}	223.06116[a]	224.26240[a]	224.67778
F_3B	C_{3v}	321.46584[a]	323.19548[a]	323.77705
CH_4	T_d	39.97688[a]	40.19517[a]	40.33244
FCH_3	C_{3v}	138.28189[a]	139.03462[a]	139.33506
F_2CH_2	C_{2v}	236.60910[a]	237.89635[a]	238.36244
F_3CH	C_{3v}	334.95172[a]	336.77164[a]	337.40456
F_4C	T_d	433.29631[a]	435.64521	436.44373
NH_3	C_{3v}	55.87220[a]	56.18436[a]	56.35371[a]
FNH_2	C_s	154.11921[a]	154.95578[a]	155.20982[a]
F_2NH	C_s	252.37543[a]	253.74316	254.24848
F_3N	C_{3v}	350.63273[a]	352.54006[a]	353.21930
OH_2	C_{2v}	75.58596[a]	76.01075[a]	76.19837
FOH	C_s	173.80067[a]	174.72958[a]	175.08480
F_2O	C_{2v}	272.01146[a]	273.45352[a]	273.98545

[a] Reference 23 (CMU archive).

$$F_2AH_2 + AH_4 \rightarrow 2FAH_3$$

$$A = \mathrm{Si},\ +8\ \mathrm{kcal/mol} \qquad (3)$$

$$A = \mathrm{C},\ +14\ \mathrm{kcal/mol}$$

$$Cl_2AH_2 + AH_4 \rightarrow 2ClAH_3$$

$$A = \mathrm{Si},\ +2\ \mathrm{kcal/mol} \qquad (4)$$

$$A = \mathrm{C},\ 0\ \mathrm{kcal/mol}$$

We present here the geometries and energies for the full set of fluorinated first- and second-row species and interpret this data with the aid of NBO analyses.

II. Methods

All computations were performed with the GAUSSIAN 82 program,[22] with use of its standard algorithms and basis sets.[2] Previous results for reference molecules were taken from the CMU Quantum Chemistry Archive.[23] Tables I and II summarize the absolute energies of first- and second-row species. All the SCF (HF) energies reported are at the optimum geometry at the SCF level for the particular basis set employed. Electron correlation corrections were probed in the frozen-core approximation by second-order Møller–Plesset perturbation theory (MP2), MP2/6-31G* energies being computed at the HF/6-31G* optimized geometries.

NBO analyses were performed with the program G82NBO,[24] which was built into link 601 of the GAUSSIAN 82 program. The total energetic importance of all electronic delocalization in the SCF wave function for a molecule can be evaluated in the NBO method by computing the energy of a single determinant composed from the doubly occupied core, lone pair, and bond NBOs that compose the NBO "Lewis structure" (the NBOs form an orthogonal set). For methane, for instance, one would evaluate the energy of the single determinant composed from the carbon core NBO and the four σ_{CH} NBOs, allowing no electron density in what are termed "Rydberg" (extravalence shell) and σ^*_{CH} NBOs. (The NBOs are held fixed, their form being that determined by our analysis of the full SCF wave function by the standard NBO procedure.) We denote the energy so determined by E(Lewis). Reoptimization of the molecular geometry with respect to E(Lewis) then reveals the influence of the delocalization on the geometry. For saturated molecules, this procedure allows a clean separation between σ and π effects. The reasonableness

---

(10) Eliel, E. L.; Allinger, N. L.; Angyal, S. J.; Morrison, G. A. *Conformational Analysis*; American Chemical Scociety: Washington, D.C. 1981. See, also: Anderson, C. B.; Sepp, D. T. *J. Org. Chem.* **1967**, *32*, 607–611.

(11) Epiotis, N. D. *Lect. Notes Chem.* **1983**, *34*, 151–185, and unpublished manuscripts.

(12) Dewar, M. J. S. *J. Am. Chem. Soc.* **1984**, *106*, 669–682.

(13) Smits, G. F.; Ph.D. Thesis, University of Leiden, 1985. Smits, G. F.; Krol, M. R.; Altona, C., to be published. See, also: Smits, G. F.; Altona, C. *Theor. Chim. Acta* **1985**, *67*, 461–475. Smits, G. F.; Krol, M. C.; van der Hart, W. J.; Altona, C. *Mol. Phys.* **1986**, *59*, 209–225.

(14) Whangbo, M.-H.; Wolfe, S. *Can. J. Chem.* **1976**, *54*, 963–968, and references therein. See ref 9b for a later quantitative study by these authors.

(15) Streitwieser, A., Jr.; Berke, C. M.; Schriver, G. W.; Grier, D.; Collins, J. B. *Tetrahedron Suppl. 1* **1981**, *37*, 345–358.

(16) Smart, B. E. *Molecular Structure and Energetics*; Liebman, J. F., Greenberg, A., Eds.; VCH: Deerfield Beach, FL, 1986; Vol. 3, pp 141–148.

(17) Dixon, D. A.; Fukunaga, T.; Smart, B. E. *J. Am. Chem. Soc.* **1986**, *108*, 4027–4031.

(18) (a) Foster, J. P.; Weinhold, F. *J. Am. Chem. Soc.* **1980**, *102*, 7211–7218. (b) Reed, A. E.; Weinstock, R. B.; Weinhold, F. *J. Chem. Phys.* **1985**, *83*, 735–746. See ref 34 for a briefer description of the natural population analysis (NPA) method. (c) Reed, A. E.; Weinhold, F. *J. Chem. Phys.* **1985**, *83*, 1736–1740.

(19) Benson, S. W. *Angew. Chem., Int. Ed. Engl.* **1978**, *17*, 812–819.

(20) Schlegel, H. B. *J. Phys. Chem.* **1984**, *88*, 6254–6258.

(21) Ho, P.; Coltrain, M. E.; Binkley, J. S.; Mellius, C. F. *J. Phys. Chem.* **1985**, *89*, 4647–4654.

(22) Binkley, J. S.; Frisch, M. J.; DeFrees, D. J.; Raghavachari, K.; Whiteside, R. A.; Schlegel, H. B.; Fluder, E. M.; Pople, J. A. GAUSSIAN 82 (release H version), Carnegie-Mellon University, 1983.

(23) Whiteside, R. A.; Frisch, M. J.; Pople, J. A. *The Carnegie-Mellon Quantum Chemistry Archive*, 3rd ed.; Carnegie-Mellon University: 1983.

(24) Reed, A. E.; Weinhold, F. *QCPE Bull.* **1985**, *5*, 141–142.

Table II. Absolute Energies (–au) of Second-Row F_nAH_m Species

species	point group	3-21G//3-21G	3-21G(*)//3-21G(*)	6-31G*//6-31G*	MP2/6-31G*//6-31G*
MgH_2	$D_{\infty h}$	199.58136[a]	199.60341[a]	200.71557[a]	200.74874[a]
FMgH	$C_{\infty v}$	297.98776[a]	298.03999[a]	299.66063	299.86901
F_2Mg	$D_{\infty h}$	396.38955[a]	396.47540	398.60243	398.98582
AlH_3	D_{3h}	242.28411[a]	242.34374[a]	243.61626[a]	243.66930[a]
$FAlH_2$	C_{2v}	340.70113[a]	340.77862	342.56333	342.78984
F_2AlH	C_{2v}	439.11683	439.21228	441.51019	441.91010
F_3Al	D_{3h}	537.52326	537.63844	540.45045	541.02240
SiH_4	T_d	289.68698[a,b]	289.78426[a]	291.22513[a,b]	291.30703[a,b]
$FSiH_3$	C_{3v}	388.07406[a,b]	388.19333[a]	390.14840[b]	390.39970[b]
F_2SiH_2	C_{2v}	486.47324[b]		489.08181[b]	489.50469[b]
F_3SiH	C_{3v}	584.87584[b]		588.01833[b]	588.61291[b]
F_4Si	T_d	683.27208[b]		686.94984[b]	687.71445[b]
PH_3	C_{3v}	340.70452[a]	340.81399[a]	342.44796[a]	342.55151[a]
FPH_2	C_s	439.03771[a]	439.16500[a]	441.32019	441.59251
F_2PH	C_s	537.39505	537.54141	540.21476	540.65977
F_3P	C_{3v}	635.77505[a]	635.94079	639.12923	639.74945
SH_2	C_{2v}	396.70467[a]	396.81964[a]	398.66732[a]	398.78821[a]
FSH	C_s	494.98460[a]	495.10751[a]	497.47930	497.77105[a]
F_2S	C_{2v}	593.28401[a]	593.41887	596.31220	596.77970

[a] Reference 23 (CMU archive). [b] Reference 20.

Table III. Stabilization Energies (Eq 5, in kcal/mol) at Various Theoretical Levels

species	3-21G	3-21G(*)	6-31G*	MP2/6-31G*[a]	other
F_2Be	–8.90		–6.66	–8.54	
F_2BH	+3.11		5.11	+3.82	
F_3B	0.12		5.71	1.02	
F_2CH_2	13.93		13.99	15.54	13.6,[b] 16.87[c]
F_3CH	37.53		36.48	40.32	32.7,[b] 40.58[c]
F_4C	62.37		57.88	63.26	50.4[b]
F_2NH	5.78		10.00	12.90	
F_3N	12.23		26.00	34.05	
F_2O	2.46		3.20	8.92	5 ± 3[d]
F_2Mg	–2.89	–0.73	–1.38	–2.17	
F_2AlH	–0.83	–0.80	–0.13	–0.18	
F_3Al	–6.65	–6.24	–4.41	–5.35	
F_2SiH_2	7.59		6.36	7.73	
F_3SiH	17.33		14.68	17.49	
F_4Si	23.08		19.85	23.05	
F_2PH	15.15	15.94	14.04	16.48	
F_3P	44.53	46.29	40.49	47.23	
F_2S	12.22	14.74	13.26	16.20	

[a] HF/6-31G* geometry used. [b] Experimental, see ref 26, corrected for zero-point energy differences. [c] HF/6-311G* level. [d] Experimental ref 19.

of this NBO approach to studying delocalization effects on molecular geometry has been tested critically in a study on $FSNH_2$,[25] a species where the major hyperconjugative (n_N–σ^*_{SF}) interaction can be physically "turned off" by internal rotation.

III. Results

A. Stabilization Energies. Table III and Figure 1 summarize the stabilization energies for all the polyfluorinated species F_nAH_m at various theoretical levels, according to eq 5. The split valence

$$F_nAH_m + (n-1)AH_{m+n} \rightarrow nFAH_{m+n-1} \qquad (5)$$

3-21G basis already gives satisfactory results. Addition of d-functions to the second-row atoms alone (3-21G$^{(*)}$) or to all heavy atoms, using in addition a better set of sp functions (6-31G*), provides refinements which are generally quite modest except when many lone pair electrons on first-row atoms are involved. From Table III it is seen that correlation enhances the stabilization energies of all polyfluorinated species except those of Be, B, Mg, and Al and that this stabilization enhancement increases with the number of fluorines present, being as much as 8 kcal/mol in NF_3. Schlegel[20] has noted the relative insensitivity in his SiH_mF_n evaluations to the level of theory employed. The agreement with

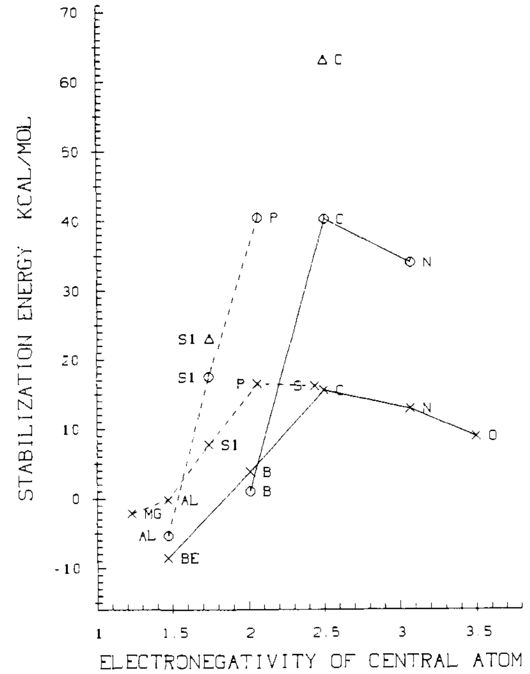

Figure 1. MP2/6-31G*//HF/6-31G* stabilization energies from Table III plotted against Allred–Rochow electronegativity of central atom for F_2AH_m (×), F_3AH_{m-1} (○), and F_4A (△) species, in kcal/mol.

experimental stabilization energies in the fluoromethane series, as noted previously by Wiberg,[26] is satisfactory. Besides this, very little additional experimental data is available (Table III) for comparison with our calculations, but it appears that the MP2/6-31G* stabilization energies may be overestimated somewhat.

Very large (over 10 kcal/mol) stabilizing interactions between geminal fluorines are found in F_2NH, F_2S, F_2PH as well as in F_2CH_2. When three fluorines are present, the stabilization in F_3P (47 kcal/mol, at MP2/6-31G*) exceeds that in F_3CH (40 kcal/mol). The magnitude in F_3N (34 kcal/mol) is also quite large, despite the difficulties which might have been anticipated from lone pair repulsion effects. Stabilizations in F_3SiH and F_4Si, while appreciable, are smaller than in their carbon counterparts, F_3CH and F_4C.

The behavior of the molecules with electropositive central A groups, (Table III; Figure 1) stands in contrast. Only F_2BH and F_3B show positive stabilization energies (1–4 kcal/mol). However,

---

(25) Reed, A. E.; Schleyer, P. v. R. *J. Am. Chem. Soc.*, submitted for publication.

(26) Wiberg, K. B., to be published.

Table IV. 6-31G* (and Experimental) Geometries of F_nAH_m Molecules[a,b]

molecule	point group	A–F	A–H	FAF	FAH	HAH
F_2Be	$D_{\infty h}$	1.371		180.0		
		(1.40 ± 0.03)			(180.0)	
FBeH	$C_{\infty v}$	1.366	1.332		180.0	
BeH_2	$D_{\infty h}$		1.334			180.0
F_3B	D_{3h}	1.301		120.0		
		(1.307)		(120.0)		
F_2BH	C_{2v}	(1.306	1.180	118.2	120.9	
		(1.311)	(1.189)	(118.3)	(120.9)	
FBH_2	C_{2v}	1.312	1.188		118.2	123.6
BH_3	D_{3h}		1.188			120.0
F_4C	T_d	1.302		109.5		
		(1.320)		(109.5)		
F_3CH	C_{3v}	1.317	1.074	108.5	110.4	
		(1.332)	(1.098)	(108.8)	(110.1)	
F_2CH_2	C_{2v}	1.338	1.078	108.6	108.9	112.5
		(1.357)	(1.093)	(108.3)	(108.7)	(113.7)
FCH_3	C_{3v}	1.365	1.082		109.1	109.8
		(1.383)	(1.100)		(108.3)	(110.6)
CH_4	T_d		1.084			109.5
F_3N	C_{3v}	1.328		102.7		
		(1.371)		(102.9)		
F_2NH	C_s	1.353	1.004	103.6	101.7	
		(1.400)	(1.026)	(102.9)	(99.8)	
FNH_2	C_s	1.386	1.003		102.4	106.6
NH_3	C_{3v}		1.002			107.2
			(1.012)			(106.7)
F_2O	C_{2v}	1.348		103.3		
		(1.405)		(103.1)		
FOH	C_s	1.378	0.952		99.80	
		(1.442)	(0.966)		(96.8)	
OH_2	C_{2v}		0.947			105.5
			(0.958)			(104.5)
F_2Mg	$D_{\infty h}$	1.723		180.0		
		(1.77 ± 0.02)		(158)		
FMgH	$C_{\infty v}$	1.729	1.705		180.0	
MgH_2	$D_{\infty h}$		1.718			180.0
F_3Al	D_{3h}	1.620		120.0		
		(1.63 ± 0.01)		(120.0)		
F_2AlH	C_{2v}	1.630	1.559	117.2	121.4	
$FAlH_2$	C_{2v}	1.640	1.574		117.6	124.9
AlH_3	D_{3h}		1.584			120.0
F_4Si[d]	T_d	1.557		109.5		
		(1.552)		(109.5)		
F_3SiH[c]	C_{3v}	1.569	1.449	108.0	110.9	
		(1.562)	(1.447)	(108.3)	(110.6)	
F_2SiH_2[c]	C_{2v}	1.581	1.461	107.6	108.9	113.4
		(1.577)	(1.471)	(107.9)	(109.2)	(112.0)
$FSiH_3$	C_{3v}	1.594	1.470		108.8	110.1
		(1.593)	(1.486)		(108.5)	(110.4)
SiH_4	T_d		1.475			109.5
			(1.481)			(109.5)
F_3P	C_{3v}	1.564		97.3		
		(1.563)		(97.7)		
F_2PH	C_s	1.580	1.402	98.8	96.6	
		(1.582)	(1.412)	(99.0)	(96.3)	
FPH_2	C_s	1.599	1.403		98.6	93.7
PH_3	C_{3v}		1.403			95.4
			(1.420)			(93.3)
F_2S	C_{2v}	1.586		97.9		
		(1.589)		(98.3)		
FSH	C_s	1.612	1.325		96.3	
HSH	C_{2v}		1.326			94.3
			(1.344)			(92.2)

[a] Distances in Å, angles in deg. [b] Experimental (generally microwave) data given in parentheses. Effective values from Harmony et al. (Harmony, M. D.; Laurie, V. W.; Kuczkowski, R. L.; Schwendeman, R. H.; Ramsay, D. A.; Lovas, E. J.; Lafferty, W. J.; Maki, A. G. *J. Phys. Chem. Ref. Data* **1979**, *8*, 619–671) were chosen, except when equilibrium values were available. Other data were taken from the JANAF Tables (Chase, M. W., Jr.; Curnutt, J. L.; Downey, J. R., Jr.; McDonald, R. A.; Syverud, A. N.; Valenzuela, E. A. *J. Phys. Chem. Ref. Data* **1982**, *11*, 695–940, and earlier supplements and editions).

this in itself is significant, since boron is a good π acceptor and fluorine is a π donor. In general, one excepts such π stabilizing interactions to fall off in magnitude as more π donor groups are added to the central atom. For example, the attenuation of substituent effects in stabilizing the isoelectronic carbocations, e.g., by sequential introduction of methyl or other groups, is well known. This is illustrated in Table III by the negative values for F_2Mg, F_3Al, and particularly for F_2Be. The Be–F bond is very strong and has significant π character. Two fluorine substituents do not provide, on average, the same degree of stabilization as a single fluorine. Thus, one surmizes that the anomeric interactions in F_2BH and in F_3B are underestimated by the energies

Table V. Optimized Geometries with Respect to *E*(Lewis)[a,c]

species	A–F	A–H	FAF	FAH	HAH	E[b]
F_4C	1.416					−435.16833
	(+0.114)					(+299.24)
F_3CH	1.427	1.002	106.6	112.2		−366.49768
	(+0.110)	(−0.072)	(−1.9)	(+1.8)		(+171.91)
F_2CH_2	1.452	1.030	103.8	107.2	122.6	−237.75978
	(+0.114)	(−0.048)	(−4.8)	(−1.7)	(+10.1)	(+85.70)
FCH_3	1.488	1.062		103.2	115.1	−138.98606
	(+0.123)	(−0.020)		(−5.9)	(+5.3)	(+30.47)
CH_4		1.095				−40.18740
		(+0.011)				(+4.88)
F_3N	1.436		95.7			−352.35845
	(+0.108)		(−7.0)			(+113.96)
F_2NH	1.449	0.982	96.5	95.4		−253.65857
	(+0.096)	(−0.022)	(−7.1)	(−6.3)		(+53.08)
FNH_2	1.469	0.993		96.0	107.2	−154.92798
	(+0.081)	(−0.010)		(−6.4)	(+0.6)	(+17.44)
NH_3		1.003			108.3	−56.18068
		(+0.001)			(+1.1)	(+2.31)
F_2O	1.408		97.1			−273.40323
	(+0.060)		(−6.2)			(+31.57)
FOH	1.421	0.947		95.0		−174.71510
	(+0.043)	(−0.005)		(−4.8)		(+9.09)
OH_2		0.946			105.9	−76.00820
		(−0.002)			(+0.4)	(+1.60)
F_3P	1.692		92.9			−638.92590
	(+0.128)		(−4.4)			(+127.59)
H_3P		1.406			93.4	−342.43496
		(+0.003)			(−2.0)	(+8.16)
F_2S	1.681		92.8			−596.23706
	(+0.095)		(−5.1)			(+47.15)
SH_2		1.331			92.7	−398.66137
		(+0.005)			(−1.6)	(+3.73)

[a] *E*(Lewis) is the energy of the NBO Lewis structure, as explained in the text. [b] The optimized values of *E*(Lewis) are given in au, corresponding to $E_L(R_L)$. The parenthesized values are the energy increase caused by forcing the wave function to be a localized Lewis structure, being $E_L(R_L) - E_F(R_F)$, in kcal/mol (see text for definitions). [c] Changes from the full SCF geometries are given in parentheses. (All computations at HF/6-31G* level.)

given in Table III. The essentially ionic compounds, F_2Mg, F_2AlH, and F_3Al, show no significant stabilization according to eq 5.

B. Geometries. In Table IV we summarize the geometries of the F_nAH_m species, giving for brevity only the parameters at our highest theoretical level, HF/6-31G*. Experimental values, where available, are given in parentheses. Comparison shows that the 6-31G* basis gives excellent geometries for second-row molecules but tends to underestimate the bond lengths when first-row lone pairs are involved. Nevertheless, these small errors appear to be systematic, and reliable conclusions can still be drawn. Brockway's effect of bond shortening with sequential fluorine substitution is observed for systems exhibiting large interaction energies (e.g., ca. 0.06 Å for nitrogen and carbon centers, ca. 0.04 Å for silicon and oxygen centers, and 0.03 Å for those involving phosphorus and sulfur). In contrast, little change in AF bond lengths is found for magnesium, aluminum, and boron. F_2Be actually is predicted to have a longer BeF bond length than in FBeH. Figure 2 depicts the variation of the AF bond contraction with respect to the electronegativity of A.

The FAF bond angles (where these are not determined by symmetry) are also of interest, for instance the long known reduction of the FCF angle (108.6°) in F_2CH_2 below the tetrahedral value. The analogous reduction in F_2SiH_2 (107.6°) is even larger. Paradoxically, the FAF angles in NF_3 and OF_2 are less than the HAH angles in NH_3 and OH_2, but the reverse is true in the second-row counterparts, PF_3/PH_3 and SF_2/SH_2, which have larger FAF than HAH angles. We shall see that much light is shed on the origin of these bond length and angle effects through NBO analysis.

Table VI. Decomposition of Stabilization Energies by NBO Energetic Analysis, HF/6-31G* Level, for Progressive Substitution[a]

reaction	ΔE	=	ΔE_L	+	ΔE_D
$CH_2F_2 + CH_4 \rightarrow 2CH_3F$	+14.0		−15.6		+29.6
$CHF_3 + CH_3F \rightarrow 2CH_2F_2$	+8.5		−22.5		+31.0
$CF_4 + CH_2F_2 \rightarrow 2CHF_3$	−1.1		−42.2		+41.1
$NHF_2 + NH_3 \rightarrow 2NH_2F$	+10.0		−10.5		+20.5
$NF_3 + NH_2F \rightarrow 2NHF_2$	+6.0		−19.3		+25.2
$OF_2 + OH_2 \rightarrow 2FOH$	+3.2		−11.8		+15.0

[a] Each of the reactions represents a loss of two $n_F \rightarrow \sigma^*_{AF}$ interactions, the total SCF ΔE is decomposed into localized NBO Lewis structure (ΔE_L) and NBO delocalization (ΔE_D) terms.

IV. Natural Bond Orbital Analysis and Discussion

A. Geometries and Energies in Absence of Delocalization. In NBO analysis, the molecular wave function is described by a set of optimum localized bond and lone pair orbitals. Departures from an ideal Lewis structure are seen as nonzero occupancies of antibond and Rydberg NBOs. We therefore have the opportunity to *restrict* the MO wave function to have the form of a Lewis structure, allowing the computation of stabilization energies and geometries in the absence of delocalization. We abbreviate the energy of the localized NBO Lewis structure, *E*(Lewis) as E_L, and denote the geometry at which E_L is minimized as R_L (representing the full set of optimized bond length and angle parameters). Denoting the full SCF energy and optimized geometry as E_F and R_F, we can express the net delocalization energy E_D as

$$E_D = E_F(R_F) - E_L(R_L) \qquad (6)$$

As no analytic expression can be written for the gradient of E_L, R_L must be optimized through single point calculations. We have therefore optimized R_L for only a subset of the species, restricting ourselves primarily to the fluorides of C, N, and O, with additional calculations on PF_3 and SF_2 to analyze the factors contributing to the bond angles of these species. The optimized R_L structures and E_L (R_L) energies (6-31G* basis set) are given in Table V, the parenthesized energies in the table being equal to the negative of E_D (in kcal/mol). The effect of delocalization on the fluorine substitution stabilization energies is presented in Table VI. As an aid in the comparison of the results in Table VI, the reaction energies given are for reactions in each of which two n_F–σ^*_{AF}

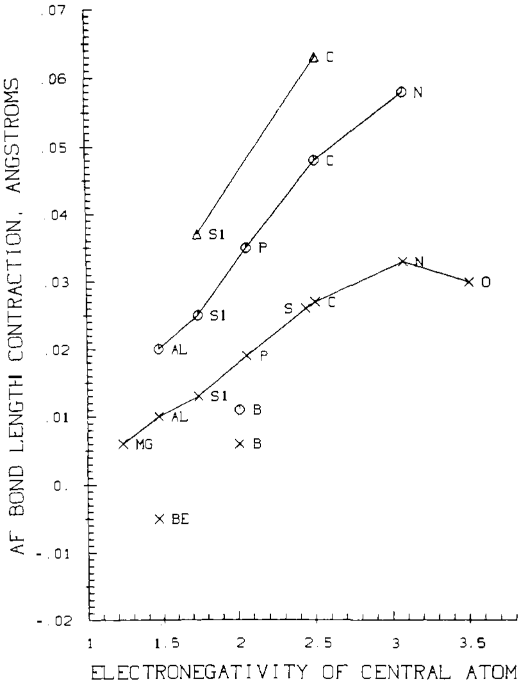

Figure 2. AF bond length changes (in Å) on going from FAH_m to F_2AH_{m-1} (×), to F_3AH_{m-2} (○), and to F_4A (△), from HF/6-31G* geometries, plotted against Allred–Rochow electronegativity of central atom A.

interactions are lost. Denoting the stabilization energies of Table III and eq 5 as E_S, the energies ΔE in Table VI are equal to $\Delta\Delta E_S$, the *second* change of E_S with respect to increased fluorine substitution.

Table VI shows that with respect to the energy of *localized* Lewis structures geminal F···F interactions are destabilizing but that the energy gains due to delocalization are sufficiently large to render the geminal F···F interactions strongly stabilizing (at least at C, N, and O centers). The destabilizing interaction in the bare Lewis structures is understandable as, for instance, the F···F distance in CF_4 is only 2.13 Å. Since we find from our analysis that the dominant contributions to the ΔE_D values in Table VI are from n_F–σ^*_{AF} interactions, these results confirm the traditional negative hyperconjugation explanation of the *energetic* anomeric effect in polyfluorinated species. Similar conclusions were reached previously by Wolfe et al.[9b] through a quantitative PMO analysis.

What about the bond length variations? Table V shows that A–F bonds are lengthened considerably (by 0.04–0.13 Å) when delocalization effects are removed. This is consistent with the negative hyperconjugation model, wherein the AF bonds acquire π-character. These bond lengthenings occur not only in the polyfluorides but also in the monofluorides, where only the weaker n_F–σ^*_{AH} type of hyperconjugation is present. This indication of significant $n_F \rightarrow \sigma^*_{AH}$ interactions is consistent with the physical evidence presented by Bent[27] for significant negative hyperconjugation in CH_3F and the experimental and theoretical findings of DeFrees et al.[28] that hyperconjugation involving methyl groups is significant in methyl-substituted anions (also see ref 25). Now, in the polyfluorides, hyperconjugation not only increases the AF π-bond order but also decreases the AF σ-bond order through the donation of charge into σ^*_{AF} orbitals. With increasing fluorine substitution, the net effect of the hyperconjugation on the variation in AF bond lengths is thus hard to predict. For the fluoromethane series, Table V indicates that the two effects roughly cancel against each other: the R_L structures show about the same CF bond length contraction from CH_3F to CF_4 as do the R_F structures of Table IV. Hence, *the bond length contraction in the series is caused by the cumulative electrostatic effect of charge withdrawal from the carbon to the fluorines.* This charge withdrawal is illustrated by the natural charges on carbon in CH_3F and CF_4 of −0.08 and +1.62, respectively. This is consistent with the results of Hehre and Pople,[9a] who found that the optimum Slater exponent for the carbon valence shell increases on going from CH_4 (1.76) to CH_3F (1.79) to CH_2F_2 (1.82) to CHF_3 (1.83) to CF_4 (1.84). A "saturation effect" is seen both in these values and in the progressively smaller bond length contractions with greater fluorine substitution in Table IV. In the nitrogen and oxygen fluorides, however, the AF bond length contraction in the R_L structures is only around half of that in the R_F structures. The NBO analysis thus ascribes around 60% of the NF bond contraction from NH_2F to NF_3 and 40% of the OF contraction from FOH to F_2O to electrostatic effects.

Interestingly, Baird[29] found that the bond length contraction in the fluoromethane series is very poorly described by the minimal STO-3G basis set which does not allow the valence shells of each atom to expand or contract with environment significantly. By contrast, this contraction is well described in split-valence basis sets, d-orbitals not being influential.[29] This provides further support for an electrostatic model of the bond length contraction. Since the energetic stabilization effect in the fluoromethanes has its origin in orbital *interactions* (hyperconjugation) and not orbital *contraction*, it appears strongly at the STO-3G basis set level[29] (indeed, due to the large basis set superposition error, the effect is strongly overestimated). Finally, it is interesting to note that the semiempirical MNDO method gives no bond length contraction *and* practically no energetic stabilization in the fluoromethane series.[29] Caution must thus be exercised in interpreting the results of MNDO calculations for systems where anomeric effects could be important.

B. Second-Order Energy Analysis. Tables V and VI represent the changes in molecular geometries and energies that occur when *all* delocalization is deleted from the wave function. Through a second-order perturbative analysis of the Fock matrix in the NBO basis, one can study the relative importance of various *individual* delocalizations. As we shall see, this is particularly useful in elucidating the origins of the angular effects in Table V: the R_L structures have considerably smaller FAF angles than the R_F structures. The second-order energy stabilization due to the localization of orbital i into orbital j is (for doubly occupied orbitals) given by eq 7. The elements F_{ij} of the Fock matrix are

$$\Delta E_{ij}^{(2)} = -\frac{2F_{ij}^2}{\Delta\epsilon_{ij}}, \qquad \Delta\epsilon_{ij} = \epsilon_j - \epsilon_i \qquad (7)$$

roughly proportional to (and generally of the same order of magnitude as) the corresponding overlap matrix elements S_{ij}, as we shall discuss in section III/E. Let us first consider the fluoromethanes. The second-order energies for single $n_F \rightarrow \sigma^*_{CH}$ and $n_F \rightarrow \sigma^*_{CF}$ stabilizations are very nearly constant throughout the whole series, having values of around −9 and −20.5 kcal/mol, respectively. The n_F–σ^*_{CF} interactions are larger partly due to a lower $\Delta\epsilon_{ij}$ (1.18 versus 1.36 au) but mainly by virtue of a much larger F_{ij}^2 (0.020 versus 0.010 au^2), a consequence of the reversed polarity of σ^*_{CF} NBOs (75% toward C) versus σ^*_{CH} NBOs (42% toward C). Now, each of the fluorocarbon reactions in Table VI represents the replacement of two $n_F \rightarrow \sigma^*_{CF}$ with two $n_F \rightarrow \sigma^*_{CH}$ interactions. The second-order estimate of the energy change with respect to negative hyperconjugation is then 2(20.5 − 9.0) = 23 kcal/mol. Note that all of the ΔE_D values in Table VI for this series are above this value. Beyond the $n \rightarrow \sigma^*$ interactions, the only other delocalizations of significance are those of $n_F \rightarrow r_C$ type, where r_C is a carbon Rydberg orbital. A detailed analysis of all second-order energy contributions reveals that the portion of the ΔE_D values beyond that which can be attributed to $n \rightarrow \sigma^*$ effects are associated with an increased strength of n_F–r_C interactions with increased fluorine substitution. In particular, the large increase of 10 kcal/mol in ΔE_D on going from the CHF_3 to the

---

(27) Bent, H. A. *Chem. Rev.* **1968**, *68*, 587–648 (see, in particular, p 634).

(28) DeFrees, D. J.; Bartmess, J. E.; Kim, J. K.; McIver, R. T., Jr.; Hehre, W. J. *J. Am. Chem. Soc.* **1977**, *99*, 6451–6452. See, also: ref 30a.

(29) Baird, N. C. *Can. J. Chem.* **1983**, *61*, 1567–1572.

CF_4 reaction is attributable to the especially strong n_F–r_C interactions in CF_4. These primarily involve donation from σ-type fluorine lone pairs into p-type carbon Rydberg orbitals.

In the fluorides of nitrogen and oxygen, the ΔE_D values can again be accounted for primarily by the n_F–σ^*_{AF} interactions; Rydberg orbitals are less significant. Note the progressive decrease of ΔE_D for the reaction energies of CH_2F_2, NHF_2, and OF_2 in Table VI, this being due to the progressively smaller polarization of σ^*_{AF} toward atom A (75 versus 66 versus 57%, respectively).

C. Bond Angle Effects. What is the angular dependence of negative hyperconjugation? The small FAF and large HAH angles in Table V are quite striking. The R_L structures have certain similarities with those of the corresponding radicals in which one fluorine has been removed, where little or no hyperconjugation is taking place, e.g., CH_3F, with R_L HCH and FCH angles of 115.1 and 103.2°, is reminiscent of the planar CH_3 radical (here, the fluorine atom bonds along the D_{3h} axis of CH_3, preferentially with a carbon hybrid of high p-character) and CH_2F_2, with R_L HCH and FCH angles of 122.6 and 107.2°, is analogous to the CH_2F radical, which has fully optimized HCH and FCH angles of 121.3 and 114.0° (UHF/6-31G*).[23] Apparently, the strong hyperconjugative delocalization from the fluorine lone pairs favors increased FAH and FAF bond angles. This is the opposite of what one might suppose on the basis that the $n_F \rightarrow \sigma^*_{AX}$ interaction (the essence of which involves partial π-bond formation between parallel p-orbitals on atoms F and A) should be strongest when the acceptor σ^* orbital is parallel to the donating π_F orbital, i.e., when the FAX bond angle is 90°. This expectation fails due to the neglect of the negative, cancelling overlap of the lone pair with the contribution to σ^*_{AX} orbital from the bonding hybrid on atom X.[30] This qualitative explanation is supported quantitatively by our detailed analysis of CH_3F presented in the Appendix. We find that negative hyperconjugation can favor smaller bond angles in very ionic species, where the lobe on X of the σ^*_{AX} orbital is very small.

These same bond angle effects are observed in the divalent and trivalent species in Table V as well. In particular, light is shed on the "mystery" concerning why PF_3 and SF_2 have significantly larger bond angles than PH_3 and SH_2, respectively, implicating hyperconjugation as the origin of the effect. All in all, the results of Table V point to an interesting interpretation of the origin of deviations of bond angles in polyfluorides from "ideal" values. In the absence of hyperconjugation, the FAF (and FAH) angles are significantly closer to 90° than in the experimental structures, revealing a strong drive toward using hybrids of high p-character at A in A–F bonds. Hyperconjugation then opens these angles significantly back toward tetrahedral values. We discuss the relationship between bond angle and hybridization further in section IV/G.

D. π-Attenuation Effects. In the fluorides of Be and B, there is a strong donation from the n_F orbitals of π-symmetry into the formally empty central atom π-orbitals. The magnitude of this delocalization stabilization is attenuated with increasing fluorine substitution (as mentioned above), as is shown by total populations (HF/6-31G*//6-31G*) of the central atom valence NBOs of π-symmetry: FBeH (0.051) versus F_2Be (0.086); FBH_2 (0.114) versus F_2BH (0.193) versus F_3B (0.259). Through the second-order energy estimates of the π-bonding strength, the decrease in π_{BeF} stabilization per fluorine substituent is 4 kcal/mol from FBeH to F_2Be, and the decrease in π_{BF} stabilization per F is 7 kcal/mol from FBH_2 to F_2BH and 3 kcal/mol from F_2BH to F_3B. The same general trends are also exhibited by the total π-type NBO populations at the central atom in the fluorides of Mg and Al: FMgH (0.040), F_2Mg (0.059), $FAlH_2$ (0.053), F_2AlH (0.089), and F_3Al (0.120). In the boron molecules, in contrast to the beryllium species, one of the fluorine p-type lone pairs can delocalize into σ^* orbitals. The trigonal (roughly 120°) angles in these species are, from our above study of the angular dependence of $n \rightarrow \sigma^*$ stabilizations, not at all unfavorable for such delocalizations. Examination of the detailed $E_{ij}^{(2)}$ delocalization energy estimates in the boron fluorides shows that, with increasing fluorine substitution, the increased number of $n_F \rightarrow \sigma^*_{BF}$ interactions more than compensates for the attenuation of the $\pi_F \rightarrow \pi_B$ interactions (and of course the loss of $n_F \rightarrow \sigma^*_{BH}$ interactions). Here we have an explanation for the fact that polyfluorination is destabilizing at Be (and Mg) but slightly stabilizing at B centers (cf. Table III). However, the F···F interactions at Al centers are destabilizing, due, as we shall see in the next section, to the weakness of hyperconjugation in such ionic species as the aluminum fluorides.

Table VII. Parameters from NBO Analysis Contributing to the Second-Order Estimate $E^{(2)}$ of $n_F \rightarrow \sigma^*_{AF}$ Interaction Strength, HF/6-31G* Level[a]

A	$E^{(2)}$	$\Delta\epsilon$	F_{no^*}	S_{no^*}	k	λ_A^2
Be	0.0	1.23	0.000	0.000		0.960
B	17.2	1.35	0.137	0.150	0.914	0.845
C	21.2	1.18	0.141	0.143	0.989	0.746
N	16.7	1.08	0.120	0.118	1.017	0.663
O	13.0	1.03	0.103	0.098	1.056	0.572
Mg	0.0	0.86	0.000	0.000		0.979
Al	9.4	1.03	0.088	0.108	0.813	0.923
Si	14.8	1.08	0.113	0.130	0.869	0.885
P	15.0	1.04	0.112	0.126	0.889	0.847
S	15.8	0.97	0.111	0.107	1.037	0.782

[a] $E^{(2)}$ in kcal/mol, $\Delta\epsilon$ and F_{no^*} in au; see the text for definition of symbols.

E. Influence of Electronegativity on Stabilization Energies. From Figure 1, it is seen that the anomeric stabilization energy is strongest for central atoms of intermediate electronegativity (P, S, C), peaking at phosphorus. Starting from phosphorus, there is a steady decline of the stabilization energy on going toward higher electronegativity of the central atoms; the drop off is steeper when these go toward lower electronegativity. These effects are in accord with the negative hyperconjugation model; the former trend reflects the decreased polarity of the σ^*_{AF} acceptor orbital with more electronegative A, but the latter trend is found to have its origin in a more complicated interplay of factors which we shall elucidate with the help of the second-order stabilization energy formula, eq 7. It is convenient to rewrite eq 7 in a manner that exhibits the explicit dependence of $E^{(2)}$ on the orbital overlap:

$$E^{(2)} = -\frac{2k^2S_{no^*}^2}{\Delta\epsilon} \qquad (8)$$

where k is the ratio between the n_F–σ^*_{AF} Fock matrix element in the NBO basis and the corresponding overlap matrix element in the pre-NBO basis (see the Appendix). Given in Table VII are the values of $E^{(2)}$, $\Delta\epsilon$, F_{no^*}, k, and S_{no^*} for the $n_F \rightarrow \sigma^*_{AF}$ interactions in the F_2AH_m species, HF/6-31G* level, along with the square of the polarization coefficient λ_A of the σ^*_{AF} orbital on atom A. We discuss these values in turn.

The values of $\Delta\epsilon$ vary primarily according to the energy of the σ^*_{AF} orbital and hence follow the strength of the AF bonds: $\Delta\epsilon$ values are larger with first-row than with second-row atoms A and are larger when the AF bonds are very polar (BF, CF, SiF) but not too ionic (AlF) or weakly polar (OF). Variations in the F_{no^*} elements are however much more important in this series, as they have a slightly greater range than the $\Delta\epsilon$ values and are squared in the equation for $E^{(2)}$. There is a steady increase in S_{no^*} in Table VII with increased electropositivity along each row (O to B; S to Si), in line with the strong increase in λ_A^2. This trend toward greater S_{no^*} is seen to be tapering off between C and B, and S_{no^*} actually decreases from Si to Al. Apparently, the increased orbital diffuseness on the central atom A with increased electropositivity has eventually enough of a weakening influence on S_{no^*} to overcome the increased λ_A^2. Increased orbital diffuseness (and longer AF bond lengths) would explain the decrease of S_{no^*} on going from first-row to second-row atoms of similar electronegativity (from C to S, for example). The k values

---

[30] (a) Similar arguments arise in the discussion of methyl tilt, see: Pross, A.; Radom, L.; Riggs, N. V. *J. Am. Chem. Soc.* **1980**, *102*, 2253. (b) This is also discussed by Spitznagel, G. W., Ph.D. Thesis, Universität Erlangen-Nürnberg, 1985.

Table VIII. NPA/NLMO Analysis of Hybridization in the Fluoromethane Series, HF/6-31G*//HF/6-31G* Wave Functions

species	C(2s)[a]	C(2p)[a]	C, av hyp[b]	q_C[a]	q_F[a]	σ_{CH} (%s)[c]	σ_{CF} (%s)[c]
CH_4	1.165	3.691	$sp^{3.17}d^{0.007}$	−0.863		$sp^{3.17}d^{0.007}$ (24.0)	
CH_3F	1.090	2.975	$sp^{2.73}d^{0.012}$	−0.083	−0.429	$sp^{2.61}d^{0.007}$ (27.6)	$sp^{3.59}d^{0.020}$ (21.7)
CH_2F_2	0.991	2.405	$sp^{2.43}d^{0.017}$	+0.570	−0.430	$sp^{2.13}d^{0.008}$ (31.8)	$sp^{3.01}d^{0.021}$ (24.8)
CHF_3	0.855	1.966	$sp^{2.30}d^{0.026}$	+1.123	−0.421	$sp^{1.72}d^{0.007}$ (36.7)	$sp^{2.53}d^{0.020}$ (28.2)
CF_4	0.666	1.630	$sp^{2.45}d^{0.041}$	+1.620	−0.405		$sp^{2.05}d^{0.018}$ (32.6)

[a] From NPA analysis. [b] Average hybridization at C, 2s:2p:3d NPA ratios. The p-hybridization is higher in CF_4 than in CH_2F_2 and CH_3F, due to the increase in π_{CF} bonding through negative hyperconjugation (back-donation from fluorine into carbon 2p-orbitals). [c] NPA hybridizations (with %s-character in parentheses) of the σ_{CH} and σ_{CF} NLMOs.

show a monotonic increase with electronegativity along both rows (B to O; Al to S). The influence of k on $E^{(2)}$ is quite strong, as $E^{(2)}$ varies as k^2, and k^2 varies in Table VII by a factor of $(1.06/0.81)^2 = 1.7$. The decrease in k with electropositivity of A is due to the reduced potential covalent character of the partial π_{FA} bond to be formed through hyperconjugation: If A is very electropositive, little π-electron donation will occur from F to A, regardless of the strength of π_{FA} overlap.[31]

There is furthermore an additional factor that reduces the stabilization energies at electropositive centers. This has to due with the fact that A–H bonds also become strongly polarized toward H and hence $n_F \rightarrow \sigma^*_{AH}$ interactions become more competitive in strength with $n_F \rightarrow \sigma^*_{AF}$ interactions. Since $n_F \rightarrow \sigma^*_{AH}$ hyperconjugation preferentially stabilizes the *mono*fluorides, the stabilization energies of eq 5 are reduced. This factor is especially influential at silicon centers, where $n_F \rightarrow \sigma^*_{AH}$ interactions are about as strong as at carbon centers (both having $E^{(2)}$ values of 9 kcal/mol), while the $n_F \rightarrow \sigma^*_{AF}$ interactions are weaker (15 versus 21 kcal/mol by $E^{(2)}$ values). At aluminum centers, there is only a 4 kcal/mol advantage of $n_F \rightarrow \sigma^*_{AF}$ over $n_F \rightarrow \sigma^*_{AH}$ interactions.

There are thus four factors that can work against the anomeric effect at very electropositive centers: increased diffuseness of orbitals on A, decreased k (through smaller potential covalent character of the partial π_{FA} bond), increased relative strength of hyperconjugation into σ^*_{AH} orbitals, and, in certain cases such as B and Al, the π-attenuation effect. It is thus understandable that, in comparison with their first-row analogues, fluorides of P and S have larger stabilization energies (in comparison with N and O, respectively) in Table III, but fluorides of Al and Si have smaller or even negative, destabilizing values (in comparison with B and C, respectively). Nonhyperconjugative factors such as purely electrostatic interactions or exclusion repulsion will also influence the curves of Figure 1, but these factors are primarily destabilizing for the polyfluorides and act mainly to lower the curves uniformly toward smaller (or even negative) stabilization energies.

F. Influence of Electronegativity on Bond Length Contractions. A significantly different (though also systematic) dependence on central atom electronegativity is exhibited by the A–F bond length contractions in the polyfluorinated species, as seen by comparing Figure 2 with Figure 1. The bond length contractions in Figure 2 peak at nitrogen, in contrast to the energy stabilizations in Figure 1 which peak at phosphorus. With the exception of the Be and B species where the π-attenuation acts to lengthen the bonds, the dependence of the bond length contractions on electronegativity is remarkably linear between $\chi = 1$ and $\chi = 3$. Here we have additional support for an electrostatic, progressive charge-withdrawal explanation of the bond length contractions: Monofluorinated species with more electropositive central atoms A are already significantly ionic, additional charge withdrawal having a smaller effect on the covalent (cationic) radius of A. When two different substituents are present that have lone pairs, however, negative hyperconjugation can play a more important role in bond length contractions. This is dramatically illustrated by $FSNH_2$,[25] where $n_N \rightarrow \sigma^*_{SF}$ hyperconjugation alone has been shown to contract the SN bond by as much as 0.08 Å *more* than the electrostatically induced contraction alone.

The changes in the A–H bond lengths with respect to increased fluorine substitution (Table IV) are also consistent with a significant electrostatically induced bond contraction. Negative hyperconjugation can only act to lengthen A–H bonds and thus counteracts any electrostatic contraction. These two effects seem nearly to cancel one another (to within 0.005 Å) except in some of the species with more electropositive central atoms (B, Mg, Al, Si). In these cases, the hyperconjugation is weaker, and the A–H bonds contract as much as 0.015 Å due to the charge withdrawal by fluorine. As Pross and Radom[9c] have shown, electrostatic factors tend to play a stronger role in substituent effects on bond lengths when the substituent is a strong σ-acceptor (F), but hyperconjugation takes control when the substituent is a weaker σ-acceptor but stronger π-donor (N).

G. Central Atom Hybridization. The bond length contractions in the polyfluorides also make sense when one considers the central atom hybridization. Consistent with Bent's rule,[8a,c] the central atom A directs hybrid orbitals of greater p-character toward the fluorines than toward the hydrogens. However, because of the strong electron withdrawal from A to F, the p:s occupancy ratio on A decreases. The p electrons of A are of higher energy and are lost or donated more easily.[8b] Thus, by natural population analysis (NPA),[18b] the average hybridization on carbon changes from $sp^{3.17}$ in CH_4 to $sp^{2.45}$ in CF_4. A significant portion of the 2p electrons on carbon in CF_4 are involved in π_{CF}, rather than σ_{CF} bonding. Indeed, the carbon hybridization in the σ_{CF} natural localized molecular orbitals (NLMOs)[18c] is $sp^{2.05}$. The hybridizations of the σ_{CH} and σ_{CF} NLMOs in the fluoromethanes are given in Table VIII, along with the total hybridization at carbon, the carbon 2s and 2p natural populations and the atomic charges. The possible roles of charge withdrawal and increased %s hybridization on carbon in the fluorocarbon bond shortenings had been suggested by Peters,[8b] increased s-character being of course consistent with shorter bond lengths.

Peters is apparently the first to have recognized that the hybrid orbitals on a given atom need not be orthogonal to each other and thus that molecules with tetrahedral symmetry are not necessarily sp^3 hybridized at the central atom.[8b,32] Switkes et al.[33] have pointed out that the removal of the hybrid orthogonality restriction allows the hybrid orbitals to "reflect the relative s- and p-orbital energies as well as the directional nature of the bonds" and

---

(31) A technical note: It is found that the k values are much more sensitive to the AO orthogonalization method than are S_{no^*} or $\Delta\epsilon$, i.e., k is sensitive to the "bookkeeping" method which determines how the electrons of the molecular wave function are to be distributed among orbitals on the various atoms. The AO orthogonalization method employed in the NBO analysis is the NAO procedure.[18b] When the occupancy weightings employed in the NAO orthogonalization procedure are all set to one (corresponding in the notation of ref 18b to an LSL orthogonalization, "L" standing for Lōwdin, instead of the WSW orthogonalization employed in the NAO procedure), k is found to be larger and to have a weaker dependence on the electronegativity of A. Such an LSL procedure, involving a Löwdin orthogonalization of the valence AO space, is, however, unrealistic, as discussed in ref 18b, for it treats the high-occupancy, low-energy orbitals of electronegative atoms on the same footing as the low-occupancy, high-energy orbitals of electropositive atoms, unfairly dividing the overlap charge between such orbitals in an even manner (similar to Mulliken population analysis which is well known to be deficient in this regard) and not according to occupancy weights as is done in the NAO procedure. Thus, the fall off of the strength of the anomeric effect in the nearly ionic species is poorly reflected in the analysis when an occupancy-weighted orthogonalization is not carried out.

(32) Peters, D. *Tetrahedron Suppl. 2* **1963**, *19*, 143–156. Peters, D. *J. Chem. Soc.* **1963**, 2003–2014.

(33) Switkes, E.; Lipscomb, W. N.; Newton, D. *J. Am. Chem. Soc.* **1970**, *92*, 3847–3853. See, also: ref 4 of this work.

presented the first determinations of hybridization through localized molecular orbital analysis of ab initio wave functions for polyatomic molecules. In SF_6,[34] NPA/NLMO analysis yields a hybridization for the six very polar σ_{SF} NLMOs of $sp^{1.7}d^{0.16}$, much further from the ideal orthogonal hybrid value (sp^3d^2) than found here for CF_4 ($sp^{2.05}$ versus sp^3). Certain contradictions in Bent's discussion of the bonding of fluoromethanes,[8a] as pointed out by Peters,[8b] arose from the assumption that CF_4 must have the same hybridization as CH_4 (exactly sp^3) and are avoided when the hybrids are allowed to be nonorthogonal.

It is a routine assumption that central atom hybrids must be orthogonal and that the angles between the valence hybrids are strictly determined,[35] implying a strict relationship between hybridization and bond angle. While these assumptions are approximately true in some cases, we wish to emphasize that they fail for species with significant ionic or hypervalent character. Other factors such as hyperconjugation can also play a significant role in determining bond angles. Magnusson has also found reason to doubt a strict relationship between bond angle and hybridization.[36] Nevertheless, we find Bent's rule to be well satisfied in the species treated in this paper, in contradiction to Magnusson's conclusion.[36] This is shown in Table VIII and by the following sample results. NPA/NLMO analysis of FPH_2 yields hybridizations at P of $sp^{4.16}d^{0.10}$ and $sp^{5.22}d^{0.13}$ for the σ_{PH} and σ_{PF} bonds, respectively. Even though the bond angle is larger in PF_3 than in PH_3, the bonds in PF_3 have higher p-character: $sp^{4.91}d^{0.16}$ versus $sp^{4.38}d^{0.07}$. Additionally, the phosphorus lone pair has 19% more s-character in PF_3 than in PH_3: $sp^{0.43}d^{0.001}$ versus $sp^{0.96}d^{0.000}$. Thus, when a molecule such as PF_3 must "decide" whether to follow Bent's rule or to follow the strict bond angle/hybridization relationship derived on the assumption of orthogonal hybrids, the first alternative is chosen. Otherwise, the phosphorus lone pair would have more s-character in PH_3 than in PF_3 because the bond angles are 1.9° smaller in PH_3. The same trend is found for hybridization at sulfur: σ_{SF} bonds in SF_2 have much *less* s-character than σ_{SH} bonds in H_2S ($sp^{8.61}d^{0.22}$ versus $sp^{4.52}d^{0.07}$) even though the bond angle in SF_2 is 3.6° wider than that in H_2S. That Bent's rule applies so well in these species is due to the tremendous changes in average hybridization upon fluorine substitution: $sp^{2.11}$ to $sp^{0.95}$ (PH_3 to PF_3); $sp^{2.61}$ to $sp^{1.75}$ (H_2S to SF_2) by NPA analysis.

Due to the small geminal atom–atom separations (for instance, 1.6 and 2.1 Å in NH_3 and PH_3), it is likely that the bond angles are influenced by steric factors as well (i.e., Pauli repulsion between bonds and between bonds and lone pairs). This has been discussed by Kutzelnigg.[37] Steric factors play a particularly important role in comparisons of first- and second-row species, and it is pointed out that the bond angle in H_2S is much smaller than would be predicted on the basis of hybridization.[37] Thus, even in simple hydrides such as PH_3 and H_2S, where no hyperconjugation is present, the bond angle–hybridization relationship fails (though it is often a good approximation for first-row species). Our point in this work however is that the bond angle changes that occur upon fluorine substitution can be ascribed qualitatively to the interplay of two factors that act in opposition to each other: the influence of electronegative fluorine on central atom hybridization and $n_F \rightarrow \sigma^*_{AH}$, σ^*_{AF} hyperconjugation.

H. Relationship to Other Models. What is the relationship between the NBO description of negative hyperconjugation and the more traditional perturbation MO (PMO)[7] treatment? In the PMO description of CH_3F, for instance, the two degenerate π_F orbitals mix with the two degenerate $\pi^*_{CH_3}$ MOs of the methyl fragment.[38] Thus, however, is mathematically equivalent to the NBO description wherein the π_F orbitals delocalize into the three σ^*_{CH} orbitals, as each π_F orbital delocalizes into a linear combination of the σ^*_{CH} orbitals that has the same symmetry as one of the $\pi^*_{CH_3}$ orbitals. Such a $\pi \rightarrow \pi^*$ PMO description of negative hyperconjugation is however only possible when the donor lone pair is antisymmetric with respect to a reflection plane that is at least locally present in the molecule. When such a local reflection plane is not present (e.g., as in SF_2), the NBO description of the negative hyperconjugation is just as "simple" as a PMO description, particularly when only one acceptor antibond is present for each lone pair. And, even when such a local mirror plane is present, the NBO description has a useful advantage over the PMO: all possible delocalizations can be seen in the analysis simultaneously as departures from an optimal localized Lewis structure. The PMO description, by contrast, can only uncover all of the possible delocalizations by making all possible decompositions of the molecule into pairs of fragments. A useful bridge between the NBO and PMO descriptions can be built by delocalizing the Lewis structure NBOs until they become doubly occupied through the formation of natural localized molecular orbitals (NLMOs).[18c] For example, the π_F NBOs in CH_3F delocalize to the extent of 1.1% (i.e., by 0.023e) onto the CH_3 group upon formation of NLMOs, 0.5% of this into a hybrid of $pd^{0.15}$ character on carbon (pure π-character) and the other 0.6% onto a linear combination of the hydrogen 1s-orbitals of π-symmetry. In CF_4, the π_F NLMOs are more strongly delocalized (2.4%), 1.8% into a π-type carbon hybrid of $pd^{0.05}$ character and the other 0.6% onto a π-type combination of the other three fluorines. Interestingly, the π_F orbitals in CH_3F and CF_4 have about the same amount of delocalization onto the other three substituents (0.6%) but the delocalization onto the central atom is four times larger in CF_4 than in CH_3F.

The total accumulation of charge on each atom X (X = H or F) in X_3CF species due to hyperconjugation from the two π-type lone pairs of one fluorine atom thus is 0.6/100 × 2 lone pairs × 2 electrons/lone pair = 0.024e. This is in qualitative agreement with the results of Streitwieser et al.[15] for the ethyl and β-fluoroethyl anions. They also found that the amount of charge accumulation at the H or F atom trans to the lone pair is only a few hundreths of an electron and that charge accumulation at F is even somewhat smaller than at H. This finding constituted a major part of the evidence that these authors put forth against negative hyperconjugation. We see, however, from our present analysis that this "evidence" is fully consistent with the negative hyperconjugation model: Replacement of H by F at carbon results (in the β-fluoroethyl anion) primarily in a greater covalency of the partial π_{CC} bond due to the larger π-electron hole on the β-carbon due in turn to the strong electron withdrawal to fluorine. Since the σ^*_{CF} orbital is much more polarized toward C than σ^*_{CH} (75 versus 42%), a given amount of hyperconjugation into σ^*_{CX} results in much less charge buildup at X for X = F than X = H. That negative hyperconjugation usually results in total charge transfers much less than 0.10e (an exception is $FSNH_2$[25]) could be taken as evidence for the unimportance of this phenomenon.[15] Elementary perturbation theory[18b] and calculation[39] demonstrate that charge transfers of as little as 0.01e can result in chemically significant energy stabilizations of the order of 0.01 au or 6 kcal/mol. In addition, intramolecular polarization can be a *consequence* of delocalization/charge-transfer interactions, due to the fact that the delocalization interaction can be increased in strength through polarization.[40] We thus reinforce and refine our previous criticisms[1a] of the conclusions of Streitwieser et al. and of their polarization model.[15]

In this connection, it is important to point out that the quantitative, orbital interaction description of negative hyperconjugation deduced from our work shows that the "no bond resonance" model of eq 2 is only a very rough and somewhat misleading repre-

---

(34) Reed, A. E.; Weinhold, F. *J. Am. Chem. Soc.* **1986**, *108*, 3586–3593.

(35) See, for example: Bingel, W. A.; Lüttke, W. *Angew. Chem.* **1981**, *93*, 944–956. Klahn, B. *J. Mol. Struct. Theochem.* **1983**, *13*, 49–77.

(36) Magnusson, E. *J. Am. Chem. Soc.* **1984**, *106*, 1177–1185, 1185–1191.

(37) Kutzelnigg, W. *Angew. Chem.* **1984**, *96*, 262–286; *Angew. Chem., Int. Ed. Engl.* **1984**, *23*, 272–295.

(38) See, e.g., Eisenstein, O.; Anh, N. T.; Jean, Y.; Devaquet, A.; Cantacuzêne, J.; Salem, L. *Tetrahedron* **1974**, *30*, 1717–1723. Note, however, that these authors overemphasized the importance of orbital energy difference to the neglect of the more important π_F–$\pi^*_{CH_2X}$ overlap increase that occurs in going, for instance, from CH_3F to CH_2F_2. See, also: ref 9b.

(39) (a) Reed, A. E.; Weinhold, F. *J. Chem. Phys.* **1983**, *78*, 4066–4073. (b) Reed, A. E.; Weinhold, F.; Curtiss, L. A.; Pochatko, D. J. *J. Chem. Phys.* **1986**, *84*, 5687–5705.

(40) Reed, A. E. Ph.D. Thesis, University of Wisconsin-Madison, 1985, pp 107–113, 137–138.

sentation of the actual delocalization interaction.

Of the alternative explanations of the anomeric effect[10-15] only one of these has been supported by quantitative calculations.[13] We therefore comment briefly on the recent work of Smits and Altona[13] who have developed an energy decomposition analysis method involving nonorthogonal, strictly local, molecular orbitals, applying it to study the anomeric effect in XCH_2Y species. In contradiction to our results, they concluded from their analysis that the anomeric effect is mainly due to the effect of substituent electronegativity on the CX–CY destructive interference interaction, quasi-classical and delocalization energy being of less importance. The Smits–Altona analysis method suffers, however, from the same basic flaw that was previously pointed out to be exhibited by the Kitaura–Morokuma analysis,[41] namely that the antibonding orbitals of one fragment are implicitly Schmidt-orthogonalized to the occupied bond and lone pair orbitals of the other fragment.[39] All n–σ^* overlap is thus awarded to the lone pair, resulting understandably in a systematic underestimation of the stabilization energy associated with this overlap. As a result, the n–σ^* energy terms are effectively incorporated into interaction energy terms involving highly occupied orbitals only. Though Smits and Altona provide an alternative description of the anomeric effect that has its own mathematical validity, given the definitions of their energy terms, their model is much more difficult to reconcile with traditional chemical bonding concepts and is indeed (in the opinion of the present authors) misleading when interpreted in terms of these traditional concepts.[42] We therefore find the NBO/PMO model of the anomeric effect to be much more useful for chemical thinking. This model was first applied to the anomeric effect by Altona,[43] and we see no reason for abandoning it now.

On the basis of his theory of "forbiddenness reduction", Epiotis[11] attempts to explain the trends in the fluoromethane series on the basis of increasing C–F bond ionicity with progressive fluorine substitution. This is contradicted by our results in Table VIII, which show that the charge on *fluorine* is rather constant throughout the series. Also, the polarities of the NLMOs for the C–F σ-bonds (not given) are constant to within 1.1% over the entire series. The progressive increase of carbon charge with an increasing number of fluorine substituents is supported by the ESCA chemical shifts (carbon 1s electron bonding energies),[44] which increase by 11 eV in going from CH_4 to CF_4. Indeed, Figure 3 shows a linear relationship of the ESCA data with the natural charges. For calibration, localized (classical) carbocations show increases in the carbon 1s core binding energy for the formally charged carbon of only 4–5 eV with respect to corresponding neutral hydrocarbons.[45]

On the basis of purely qualitative arguments based on his MOVB diagrams, Epiotis[11] argues that CH_3F has "effective T_d symmetry" and that the fluorine atoms in CH_3F, CH_2F_2, CHF_3, and CF_4 can bond with 0, 1, 2, and 3 of the carbon 2p orbitals, respectively. Our results provide no support for these arguments. From Table VIII, the carbon hybrid that bonds with fluorine in CH_3F has the highest p-character ($sp^{3.6}$), and this *decreases* progressively along the series ending in CF_4. Furthermore, our finding in Figure 1 that stabilization is larger at P and S than at N and O, respectively, contradicts the "prediction" of Epiotis that the stabilization energies at second-row ("green") centers should be lower than at first-row ("black") centers. The convergence of the stabilization energies in Table III indicate that it is unlikely that these values will change significantly at higher basis set levels.

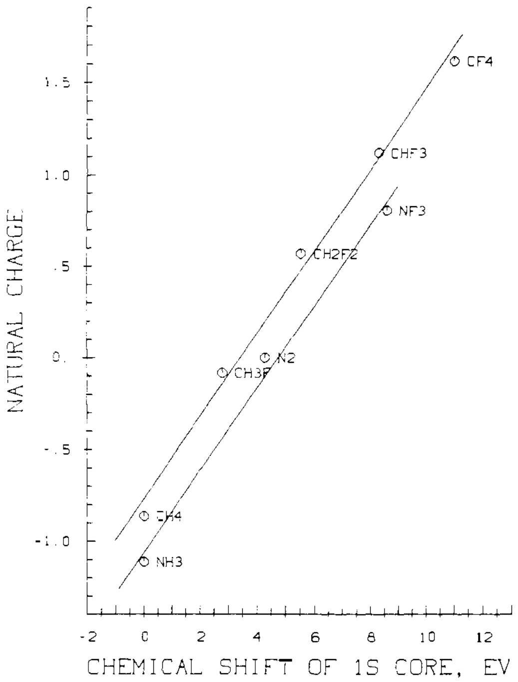

Figure 3. HF/6-31G* natural charges of the central atom plotted against experimental 1s electron bonding energies (chemical shifts, in eV, relative to CH_4 for carbon and NH_3 for nitrogen) from ref 44, for series of carbon and nitrogen species. Least-squares linear fits are drawn for each series.

I. Comparison with Other Work. All previous theoretical studies of the anomeric effect and negative hyperconjugation have involved carbon centers (i.e., A = C). Some comparison with the present work nevertheless is appropriate. Friedman et al.[46] have extended our earlier study[1a] of $HOCH_2CH_2^-$ and $F_3CCH_2^-$. On the basis of orbital and electron density plots, they found support for negative hyperconjugation of $n_C \rightarrow \sigma^*_{CX}$ type in these species. Their discussion of $F_3CCH_2^-$ is misleading, however. In this species, which is closely related to the F_3CNH_2 species (to be discussed in our next paper),[25] hyperconjugation can occur into *all* of the σ^*_{CF} orbitals that are not perpendicular to the carbon lone pair. The dihedral angle dependence of hyperconjugation in $F_3CCH_2^-$ therefore can only be very small, and there is no reason to be surprised, as were Friedman et al.,[46] that the C–C distance and total energy do not change much with internal rotation. They describe a $n_C \rightarrow \pi^*(CF_2)$ interaction in $F_3CCH_2^-$ that is said to provide a "competing stabilization mechanism" distinct from hyperconjugation! This $n_C \rightarrow \pi^*(CF_2)$ interaction is identical with $n_C \rightarrow 2\sigma^*_{CF}$ hyperconjugation, where n_C delocalizes into the antisymmetric combination of two σ^*_{CF} orbitals. A puzzling feature of the Friedman paper[46] is the plot of the HOMO of $HOCH_2CH_2^-$, which shows delocalization of n_C onto O but not onto the other C atom, as one would have expected. The explanation for this was given by Kost and Raban,[47] in a noteworthy earlier study of negative hyperconjugation. They noted a similar feature in the plot of the HOMOs of XCH_2NH_2 species and pointed out that the lobe on CH_2 in the HOMO of these species is reduced in magnitude due to mixing with other occupied MOs that have contributions from the σ_{CX} orbital.[47] This latter mixing has nothing to do with the $n \rightarrow \sigma^*_{CX}$ hyperconjugation and complicates attempts to "see" hyperconjugation in delocalized MOs. The localized orbital (NBO) approach employed in our work thus is more useful for studying orbital delocalization.

There is much current interest in anomeric effects and negative hyperconjugation involving second-row elements.[48-50] In our

---

(41) Kitaura, K.; Morokuma, K. *Int. J. Quantum Chem.* **1976**, *10*, 325–340.

(42) What we specifically mean here by "traditional bonding concepts" is the explanation of energetic stabilizations in terms of orbital delocalization interactions, wherever this is possible. The delicate but important interpretational questions touched on here and in ref 39 will be discussed more fully in the following: Reed, A. E.; Curtiss, L. A.; Weinhold, F. *Chem. Rev.* (to be published).

(43) Altona, C., Ph.D. Thesis, University of Leiden, 1964. See, also: ref 7b.

(44) Jolly, W. L.; Perry, W. B. *Inorg. Chem.* **1974**, *13*, 2686–2692.

(45) Olah, G. A.; Mateescu, G. D.; Wilson, L. A.; Gross, M. H. *J. Am. Chem. Soc.* **1970**, *92*, 7231. Olah, G. A.; Mateescu, G. D.; Riemenschneider, J. L. *J. Am. Chem. Soc.* **1972**, *94*, 2529.

(46) Friedman, D. S.; Francl, M. M.; Allen, L. C. *Tetrahedron* **1985**, *41*, 499–506.

(47) Kost, D.; Raban, M. *J. Am. Chem. Soc.* **1982**, *104*, 2960–2967.

earlier study of XCH_2Y species[1b] and in the study of Magnusson on YCH_3 and YCF_3 species,[49] it was found that negative hyperconjugation involving *lone pairs* on second-row substituents Y is much weaker than with corresponding first-row substituents. On the contrary, it is now clear from the present study that negative hyperconjugation involving *central atoms* A from the second row may be stronger than that involving corresponding first-row atoms. This is supported also by our study of the stabilization of carbanions H_2CA^- by first- and second-row substituents.[50] However, in these cases, greater polarizability of second-row atoms was an important factor as well: in $CH_3CH_2^-$ (A = CH_3), a destabilization of 3 kcal/mol with respect to CH_3^- (X = H) occurred, whereas with the roughly isoelectronic substituent A = SH, a stabilization of 21 kcal/mol in $HSCH_2^-$ was found.[50] In the present work, negative hyperconjugation is found to be roughly equal in magnitude at C and S (see Figure 1).

Further evidence for negative hyperconjugation into σ^*_{CF} orbitals is provided by studies of Dixon and co-workers.[17,51] By experiment and theory, F_3CO^- is found to have a very short C–O bond length (1.23 Å by experiment) and C–F bonds that are about 0.06 Å longer than in F_3CH. Negative hyperconjugation is thus quite strong in F_3CO^- and is consistent with the very small FCF angles observed (102°), which are around 7° less than those in saturated species. In this case, electronegativity and hyperconjugation effects work in concert to reduce FCF angles. Dixon and co-workers have examined the stabilization of CF_3^- theoretically by replacing fluorine substituents by CF_3 groups.[17] This allows $n_C \rightarrow \sigma^*_{CF}$ stabilization. Relative to CF_3^-, $(F_3C)_3C^-$ was found to be stabilized by 40.8 kcal/mol. They also found that β-fluorines stabilize carbanions more effectively than α-fluorines.[17] A word of caution is advisable, however, with regard to the estimate of Dixon and co-workers[51] that no bond resonance structures contribute roughly 20% to the bonding in F_3CO^-. As we discussed in section IV/H above, negative hyperconjugation is an orbital interaction that can be only very crudely represented by no bond resonance structures such as in (eq 2).

V. Conclusions

In this work we have not only increased the data base of ab initio energetic and geometric data concerning the anomeric effect but have also, with the aid of NBO energetic analysis, derived a refined picture concerning the interrelationship between these energetic and geometric effects and the molecular wave functions. We have found a direct connection between negative hyperconjugation and the energetic stabilizations associated with the anomeric effect. The NBO analysis aided in pictorially understanding the dependence of the energetic anomeric effect on the central atom. This is strongest when the central atom is of intermediate electronegativity but is attenuated in trigonal species by π-donation. Additionally, we have evaluated the effects of negative hyperconjugation on bond lengths and angles. The influence on bond lengths is found to be very strong, but the progressive bond length shortening in polyfluorinated species (noted by Brockway)[3] is to be primarily attributed to the increased charge withdrawal from the central atom (electrostatic contraction). The effect on bond angles is also found to be pronounced but counter intuitive: bond angles are widened so that unfavorable negative overlap between the donor lone pair and the out-of-phase part of the acceptor antibond is minimized.

Finally, it is important to point out that the results of the present work have major implications for the energies, geometries, and conformations of species where substituents other than F are attached to central atoms of intermediate electronegativity. Indeed, an anomeric effect at a tetracoordinate boron center ($n_O \rightarrow \sigma^*_{BCl}$ interaction) has recently been deduced from an X-ray structure.[52] Calculational results in $FSiH_2NH_2$ illustrate what can be expected. As in FCH_2NH_2,[1] the nitrogen lone pair and the A–F bonds are in the trans planar arrangement which favors π-donation by N into the σ* SiF orbital. The SiF bond is lengthened, and the SiN bond is shortened (versus SiH_3F and SiH_3NH_2) as a consequence. The stabilization energy (8.0 kcal/mol, 6-31G*//6-31G*) in $FSiH_2NH_2$ is appreciable but less

Table IX. Absolute Energies (–au) of Tetravalent B, N, Al, P Species

species	point group	3-21G//3-21G	6-31G*//6-31G*
BH_4^-	T_d	26.802 95	26.965 10
FBH_3^-	C_{3v}	125.209 25	125.884 71
$F_2BH_2^-$	C_{2v}	223.627 24	224.822 98
F_3BH^-	C_{3v}	322.058 78	323.773 14
F_4B^-	T_d	420.492 47	422.725 15
NH_4^+	T_d	56.233 86	56.530 77
FNH_3^+	C_{3v}	154.429 57	155.263 55
$F_2NH_2^+$	C_{2v}	252.631 58	254.011 62
F_3NH^+	C_{3v}	350.835 44	352.767 47
F_4N^+	T_d	449.036 16	451.519 39
AlH_4^-	T_d	242.877 45	244.213 30
$FAlH_3^-$	C_{3v}	341.398 42	343.164 08
$F_2AlH_2^-$	C_{2v}	439.727 83	442.121 39
F_3AlH^-	C_{3v}	538.160 77	541.081 47
F_4Al^-	T_d	636.592 04	640.039 90
PH_4^+	T_d	340.998 17	342.761 58
FPH_3^+	C_{3v}	439.312 12	441.627 48
$F_2PH_2^+$	C_{2v}	537.642 11	540.508 50
F_3PH^+	C_{3v}	635.976 59	639.394 14
F_4P^+	T_d	734.303 35	738.272 42

Table X. Stabilization Energies (Eq 5, in kcal/mol) of Tetravalent Ionic Species

species	3-21G//3-21G	6-31G*//6-31G*
$F_2BH_2^-$	7.34	11.71
F_3BH^-	23.17	30.88
F_4B^-	40.36	51.21
$F_2NH_2^+$	3.95	9.59
F_3NH^+	9.07	24.07
F_4N^+	12.21	36.08
$F_2AlH_2^-$	5.30	4.10
F_3AlH^-	12.81	9.93
F_4Al^-	19.27	14.73
$F_2PH_2^+$	10.07	9.49
F_3PH^+	22.95	21.84
F_4P^+	30.99	29.64

Table XI. HF/6-31G* Optimized Geometries of Tetravalent Ions

species	point group	A–F	A–H	FAF	FAH	HAH
BH_4^-	T_d		1.243			109.5
FBH_3^-	C_{3v}	1.440	1.248		110.3	108.6
$F_2BH_2^-$	C_{2v}	1.421	1.246	108.4	109.5	110.4
F_3BH^-	C_{3v}	1.406	1.236	108.6	110.4	
F_4B^-	T_d	1.394		109.5		
NH_4^+	T_d		1.013			109.5
FNH_3^+	C_{3v}	1.333	1.015		107.8	111.1
$F_2NH_2^+$	C_{2v}	1.308	1.018	109.0	108.4	114.2
F_3NH^+	C_{3v}	1.289	1.023	108.9	110.1	
F_4N^+	T_d	1.280		109.5		
AlH_4^-	T_d		1.651			109.5
$FAlH_3^-$	C_{3v}	1.700	1.650		109.2	109.7
$F_2AlH_2^-$	C_{2v}	1.692	1.643	107.9	109.4	111.5
F_3AlH^-	C_{3v}	1.685	1.629	108.4	110.5	
F_4Al^-	T_d	1.677		109.5		
PH_4^+	T_d		1.380			109.5
FPH_3^+	C_{3v}	1.523	1.375		108.3	110.6
$F_2PH_2^+$	C_{2v}	1.506	1.370	108.0	108.4	115.0
F_3PH^+	C_{3v}	1.491	1.364	108.0	110.9	
F_4P^+	T_d	1.480		109.5		

---

(48) See, e.g., Anet, F. A. L.; Kopelevich, M. *J. Chem. Soc., Chem. Commun.* **1987**, 595–597, and references therein.

(49) Magnusson, E. *J. Am. Chem. Soc.* **1986**, *108*, 11–16.

(50) Schleyer, P. v. R.; Clark, T.; Kos, A. J.; Spitznagel, G. W.; Rohde, C.; Arad, D.; Houk, K. N.; Rondan, N. G. *J. Am. Chem. Soc.* **1985**, *107*, 4565–4567.

(51) Farnham, W. B.; Smart, B. E.; Middleton, W. J.; Calabrese, J. C.; Dixon, D. A. *J. Am. Chem. Soc.* **1985**, *107*, 4565–4567.

(52) Shiner, C. S.; Gardner, C. N.; Haltiwanger, R. C. *J. Am. Chem. Soc.* **1985**, *107*, 7167–7172.

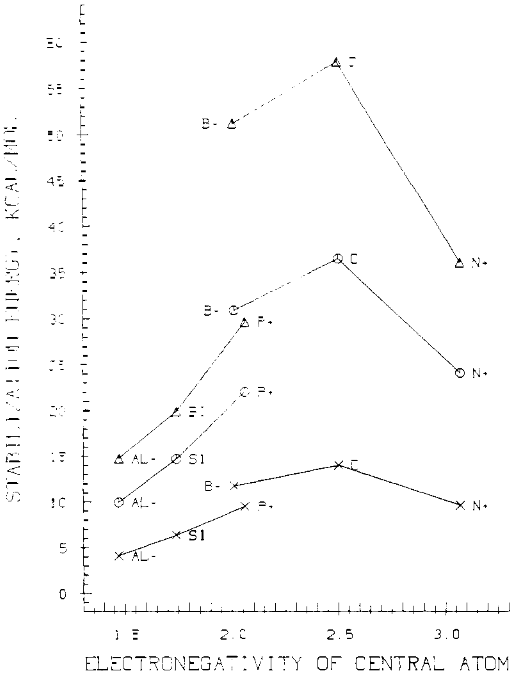

Figure 4. HF/6-31G*//HF/6-31G* stabilization energies from Tables III and X plotted against Allred–Rochow electronegativity of central atom for F_2AH_2 (×), F_3AH (○), and F_4A (△) species, in kcal/mol.

than that in the carbon analogue, FCH_2NH_2 (12.9 kcal/mol). Further details and examples will be presented in the following papers in this series.[25,53]

Acknowledgment. This work was supported by the Deutsche Forschungsgemeinschaft and the Fonds der chemischen Industrie. We thank Professor J. A. Pople and his associates who gathered the valuable data summarized in the CMU archive of which we have made liberal use. Professor N. D. Epiotis suggested that we examine $FSiH_2NH_2$ and provided stimulation. Some calculations were carried out by G. W. Spitznagel and other members of the Erlangen group. We thank Prof. C. Altona for a copy of ref 13 and discussions and Professor F. Weinhold and his group for discussions about pre-NBOs.

Appendix

We present here the details of an orbital overlap analysis of the dependence of negative hyperconjugation on FAF bond angle, in CH_3F and F_2AlH.

When the bond lengths in CH_3F are held at their R_F values and the HCF angle θ varied from 90° to 135°, one comes to the remarkable finding that negative hyperconjugation increases monotonically in magnitude with θ, as seen by the second-order energy estimates and other measures of the n_F–σ^*_{CH} interaction. This increase is directly caused by the angular dependence of the n_F–σ^*_{CH} Fock matrix elements, implying that n_F–σ^*_{CH} overlap increases with θ. We thought it desirable to study these overlap integrals directly. Since the NBOs form an orthogonal set, we must employ a corresponding nonorthogonal basis set. We therefore leave the interatomic orthogonalization steps out, replacing the NAO transformation T_N by the preorthogonal NAO ("pre-NAO") transformation, **N**.[18b] Multiplying **N** by the NAO to NBO transformation, we obtain the so-called preorthogonal NBOs ("pre-NBOs"). Additionally, it is useful to decompose the $n_F \rightarrow \sigma^*_{CH}$ pre-NBO overlap into components from the overlap of the lone pair with the individual carbon and hydrogen hybrids contributing to σ^*_{CH}, weighted by the respective polarization coefficients of the hybrids. With a 90° value of θ in CH_3F (6-31G* level), the $n_F \rightarrow \sigma^*_{CH}$ pre-NBO overlap is 0.0305, this being the sum of the carbon and hydrogen components of the overlap which are +0.1198 and −0.0893, respectively. At $\theta = 120°$, these three overlaps become $0.0840 = +0.1194 - 0.0354$. One sees a slight decrease of the carbon component of the pre-NBO overlap with θ but a rapid decrease in the magnitude of the hydrogen component of this overlap. At the R_L and R_F values of θ (103.2 and 109.1°), the total pre-NBO overlaps are 0.0611 and 0.0710 (the bond lengths being again at their R_F values). The $E^{(2)}$ estimates of a single n_F–σ^*_{CH} interaction vary with θ as follows: −2.3 (90°), −7.0 (103.2°), −8.9 (109.1°), and −11.2 (120°), in kcal/mol.

When, on the other hand, the A–F bonds are very ionic, the interference cancelation of the $n_F \rightarrow \sigma^*_{AlF}$ overlap as the FAF angle is decreased toward 90° is of much reduced importance. Indeed, in F_2AlH, the $n_F \rightarrow \sigma^*_{AlF}$ interaction increases steadily (but slowly) in magnitude as the FAlF angle is reduced from its HF/6-31G* value (117.2°) to 90°, the $E^{(2)}$ value changing from −9.4 to −10.9 kcal/mol. Negative hyperconjugation can thus favor smaller bond angles only in very ionic species.

Note Added in Proof. After this work had been already submitted, we recognized that fluorine hyperconjugation at B and Al centers could be evaluated by examining the *tetrahedral* anions, thereby avoiding the π-attenuation effects. We therefore carried out geometry optimizations on all possible tetravalent F_nAH_m species, where $A = B^-$ and Al^- as well as the cations N^+ and P^+. The total energies and stabilization energies (at HF/3-21G//HF/3-21G and HF/6-31G*//HF/6-31G*) of these species are given in Tables IX and X, respectively, and the HF/6-31G* geometries in Table XI. The results are summarized in Figure 4 where the HF/6-31G*//HF/6-31G* stabilization energies are plotted against the electronegativity of the central atom; the tetrahedral carbon and silicon species, CF_4 and SiF_4, are included for completeness. The curves peak at C for the first row and increase monotonically from Al to Si to P for the second row, consistent with our expectations. The major difference between Figure 1 and 4 is the significant (and positive) stabilization at B and Al in the latter. In addition, stabilization is somewhat greater at N than P in Figure 4, which is opposite of the situation in Figure 1. In Figure 1, if one ignores the point for B, the stabilization curves for the first- and second-row centers merge smoothly into each other. This is not the case in Figure 4, where the second-row curves are significantly lower in stabilization energy than the first-row curves. In particular, stabilization at B is much greater than at P, even though these atoms are roughly of the same electronegativity. However, these curves could be influenced by the total molecular charge, which might increase the stabilization energies at B and Al and decrease those at N and P.

Registry No. F_2Be, 7787-49-7; F_2BH, 13709-83-6; F_3B, 7637-07-2; F_2CH_2, 75-10-5; F_3CH, 75-46-7; F_4C, 75-73-0; F_2NH, 10405-27-3; F_3N, 7783-54-2; F_2O, 7783-41-7; F_2Mg, 7783-40-6; F_2AlH, 24586-56-9; F_3Al, 7784-18-1; F_2SiH_2, 13824-36-7; F_3SiH, 13465-71-9; F_4Si, 7783-61-1; F_2PH, 14984-74-8; F_3P, 7783-55-3; F_2S, 13814-25-0; FBeH, 60872-05-1; BeH_2, 7787-52-2; FBH_2, 27944-03-2; BH_3, 13283-31-3; FNH_2, 15861-05-9; FMgH, 60872-06-2; MgH_2, 7693-27-8; $FAlH_2$, 110510-76-4; AlH_3, 7784-21-6; FPH_2, 14500-81-3; FSH, 62064-82-8.

---

(53) Reed, A. E.; Schade, C.; Schleyer, P. v. R.; Kamath, P. V.; Chandrasekhar, J. *J. Chem. Soc., Chem. Commun.*, in press.